Textile & Leather Review

ISSN 2623-6281 | www.tlr-journal.com | 10.31881/TLR

Analysis of the Outer Layer Performance of Fire Protective Clothing

Rochak Rathour, Sudhanshu Maurya, Tathagata Das, Bhavna Rajput, Apurba Das, Ramasamy Alagirusamy

How to cite: Rathour R, Maurya S, Das T, Rajput B, Das A, Alagirusamy R. Analysis of the Outer Layer Performance of Fire Protective Clothing. Textile & Leather Review. 2024; 7:366-390. https://doi.org/10.31881/TLR.2023.213

How to link: https://doi.org/10.31881/TLR.2023.213

Published: 6 March 2024

Analysis of the Outer Layer Performance of Fire Protective Clothing

Rochak RATHOUR[1], Sudhanshu MAURYA[1*], Tathagata DAS[1], Bhavna RAJPUT[2], Apurba DAS[1], Ramasamy ALAGIRUSAMY[1]

[1]Department of Textile and Fiber Engineering, Indian Institute of Technology Delhi, Hauz Khas, New Delhi, India

[2]Department of Mechanical Engineering, Indian Institute of Technology Delhi, Hauz Khas, New Delhi, India
*sudhanshumaurya8@gmail.com

Article
https://doi.org/10.31881/TLR.2023.213
Received 27 December 2023; Accepted 20 February 2024; Published 6 March 2024

ABSTRACT
In the present study, an attempt has been made to analyse the protection performance of fire-protective clothing. Various exposures to the same fabric in different configurations result in different protection performances. Box-Behnken experiment design was used to optimize the process parameters such as pick density (P), heat flux (Q), and air gap (D). Through surface methodology response, the relationship among the process parameters such as pick density (P), heat flux (Q), and air gap (D) was established. The experimental multi-parametric equation for calculating the radiant protection time (R_T) and flame protection time (F_T) was acquired. The fabric used was developed with 2/40 Ne Nomex IIIA yarns. The pick density (P) ranged from 40 to 64 picks per inch, heat flux (Q) ranged from 0.5 to 1.5 cal/cm^2/sec, and air gap (D) ranged from 0 to 25 mm. To experimentally determine the level of protection, Stoll criteria were used. The experimental and predicted protection time values show a high correlation coefficient value (R^2 = 0.985 for radiant and 0.978 for flame). The maximum improvement in protection was obtained at a high level of air gap (25 mm), low level of heat flux (0.5 cal/cm^2/sec) and low level of pick density (40 picks per inch). Obtained results, calculations and equations will help researchers explore the empirical equation of the Box-Behnken model and other surface response curves. The values of protection time, in the specified range of the process parameters, by a single calculation could be possible to obtain.

KEYWORDS
fire protective clothing, fire protection performance, honeycomb woven fabric, pick density, air gap, heat flux

INTRODUCTION

The brigades of firefighters, army personnel and industrial workers often face unpredictable hazardous environments in their line of duty. The hazards could arise from one or a combination of more than one of the following elements: a poisonous fume, a toxic chemical, steam, hot liquid biological heat, etc. [1-5]. The environment prevailing in a firefighting situation depends on heat flux and ambient temperature from moderate to severe situations and the firefighting clothing is made of multilayered woven and non-woven fabrics, depending on their purpose [6-10]. These different layers may be distinguished from one another by the composition and specific properties of each layer (Figure 1). The specifications of the layered structure for occupational safety of firefighters are described below:

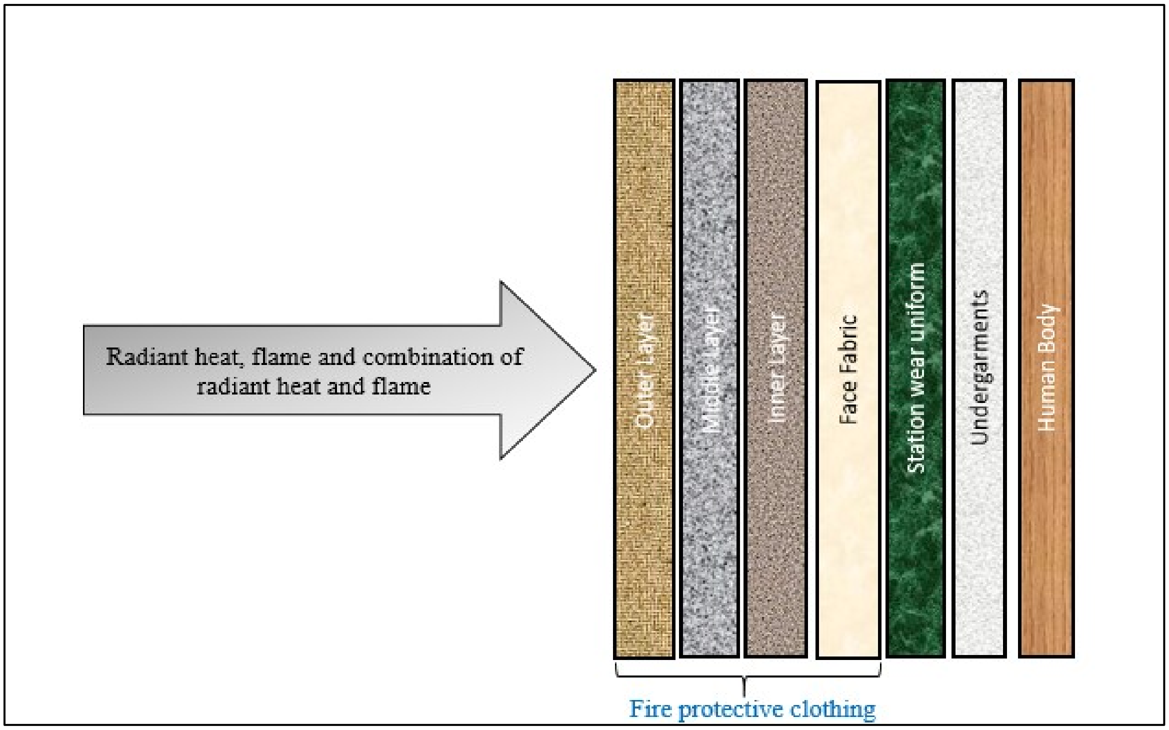

Figure 1. Schematic figure of different layers of multi-layer fire protective outfits

The external/outer layer or shell fabric is made up of flame and heat-resistant fabric which protects the user from hazardous fire injuries and imparts heat resistance, strength and durability properties [11-14]. The overall performance of fire-protective clothing is the cumulative effect of a large number of contributory factors. Some of these are fabric thickness, areal density, weave type of woven fabric (e.g. plain, twill, satin, basket etc.), construction of knitted fabrics, thermo physical properties of fabrics pyrolysis and fabric shrinkage, air gap width, types of exposure, presence of moisture, aerogel etc [15,9,10,18]. Out of these parameters thread or areal density, air gap and level of heat flux are very crucial. Barker and Shalev observed that the fire-protective performance of fabric increases with an increase in areal density [19]. Das et al., Sun et al., Kutlu and Cireli investigated the effectiveness of areal density concerning fire-protective performance and drew similar conclusions, but they considered it less significant for fire-protective clothing [20-22]. Rathour et al. analyzed the effect of different structures and pick density and they observed that a honeycomb is a better-woven structure compared to other weaves [23]. Udayraj et al. concluded that Stoll’s second-degree burn times in the case of both radiant heat and flame are directly proportional to pick density and inversely proportional to heat flux but missing the effect of air gap, low level of heat flux and high level of pick density [24]. Single-layer fabrics were subjected to exposure to radiant heat, flame and a combination of radiant heat and flame as heat sources and varying the intensity of heat flux at three different levels of 20, 40 and 84 kW/m^2 [25]. The authors observed that the thermal protective performance (TPP) of fabric increases with an increase in the areal density of fabric but a reverse effect with an increase in heat intensity. The layering of fabric structure favours the improvement in the performance of fire protection, both for radiant heat and naked flames [26]. The second-degree burn time under sub-flashover conditions is found to decline with an increase in exposure to heat flux produced by radiant heat [27]. An investigation on the effect of exposure to low intensities of thermal radiation (1, 2, 3, 5, 7 and 10 kW/m^2) on heat transfer through multilayer fire protective clothing indicated that the heat transfer is noticeably affected by the moisture transfer [20,21]. Sawcyn and Torvi designed a model to calculate the contribution of heat transfers by convection and radiation from a test specimen [30]. The author observed a rise in sensor temperature as a result of heat transfer in both cases. Talukdar et al. and Song et al. observed that an air gap between the fabric and the skin works as a second layer of insulation, slowing heat transmission to the skin [31,32]. The thickness of the fabric system has a significant impact on the performance of fire-resistant garments. A model has been described by Torvi for the measurement of heat transfer through fire-resistant fabrics during the cooling phase following exposure to fire [33]. In another investigation, Lu et al. evaluated the fire-protective performance of flame-resistant fabrics that had been subjected to exposure to intense heat at different levels of added moisture [34]. The author noted a significant improvement in fire protective performance with an increase in the amount of added moisture. Widening of the air gap produced further improvement in fire protective performance. The most effective performance is obtained with a 9-12 mm of air gap. Fu et al. analyzed the effects of multi-layered air gaps on the thermal performance of firefighter protective garments were investigated while the firefighters were exposed to low-level heat [35]. To enhance the fire-resistant properties of cellulose fabric, a novel fire-preventing triple-network (TN) hydrogel was developed and laminated on cotton fabric by Yu et al. [36]. Ultrasensitive temperature monitoring and energy harvesting in firefighting equipment were produced using a self-powered electronic textile (SFA e-textile) based on conductive aerogel fibre that comprises calcium alginate (CA), Fe_3O_4 nanoparticles (Fe_3O_4 NPs), and silver nanowires (Ag NWs) by Yu et al. [37].

Surface Response Models (SRM) including Central Composite Design, Box Behnken Design and other methods evaluate linear, quadratic, and cubic data [38]. Ba-Abbad et al. reported Box Behnken Design reduced the number of tests, saving time and money without impacting output quality [39]. The design of the experiment can overcome the one-variable-at-a-time technique's limitations, according to Srinu

Babu et al. [40-41]. Several sources propose implementing a three-level, three-factor Box Behnken design to develop empirical model equations relating output responses to process parameters [42-45].

In the present work, an approach is being investigated to determine the most appropriate combination of process parameters A (pick density), B (heat flux) and C (air gap), which is the distance between the fabric (outer layer) and the sensor (copper calorimeter) for outer layer of fire protective clothing under exposure of 10% radiant heat and 100% flame. This study will also provide scientific knowledge of the most important process parameter air gap and compactness (achieved by varying pick densities). The values of the response parameter (R_T- Radiant protection time and F_T-Flame protection time) were experimentally determined against three levels of each process parameter by using a specially designed benchtop apparatus. An empirical equation was developed to estimate the computed values of protection time using Box-Behnken DOE as a statistical tool. An attempt was also made to explain the results by creating bar charts using different combinations of variables. This is the first of its kind study reported for all three process parameters at three levels for both exposures (100% radiant heat and 100% flame) in a single paper with an empirical equation. This will also help the researchers to obtain the values in the given range of process parameters by a single calculation and how to explore the empirical equation of the Box-Behnken model and other surface response curves.

EXPERIMENTAL

Materials and methods

Materials

The fabric used in this research was created using 2-ply 40 Ne count Nomex IIIA ring spun yarns directly procured from the manufacturer (Arvind Ltd. advance materials division, Gujarat). Honeycomb 2D weave was used to weave the outer layer fabric of fire protection clothing. The fabric with honeycomb weave construction was woven on a wooden handloom of the weaver service centre, Bharat Nagar, New Delhi. The thread density in the warp direction of such fabric is constant (42 EPI means ends per inch), while the thread density in the weft direction was varied between 40, 52, and 64 picks per inch (PPI), resulting in three fabrics.

Methods

Physical properties

The properties are measured based on the following standards-

Thread Density - ASTM D3775-12, Standard Test Method for measurement of thread density of Fabric

Areal Density - ASTM D3776-09, Standard Test Method for measurement of mass per unit area of Fabric

Thickness - ASTM D1777-96, Standard Test Method for measurement of the thickness of Fabric

Air permeability - ASTM D737-96, Standard Test Method for measurement of Air permeability of Fabric

Cover factor - Describes the percentage area of the fabric covered by the yarn and measured according to the following relation.

Cloth cover factor = C1 + C2 – {(C1×C2)/28}

Where, C1 = warp cover factor = ends per inch/ (warp count (Ne) ^1/2) and

C2 = weft cover factor = picks per inch/ (weft count (Ne) ^1/2).

Protective Performance: Radiant and Flame Protective Performance Tester

As seen in Figure 2, a vertical radiant and flame protective performance tester (which are closer to the situations faced by the firefighters during operations in reality.) was used to assess the heat flux Q conveyed via an air gap D using a heating block, fabric mounting assembly, and a moving copper calorimeter. This is a benchtop test setup which is used to determine the thermal protective performance of the fabric ensembles. The bench top tests are preferred as they are easily accessible, efficient and easy to operate.

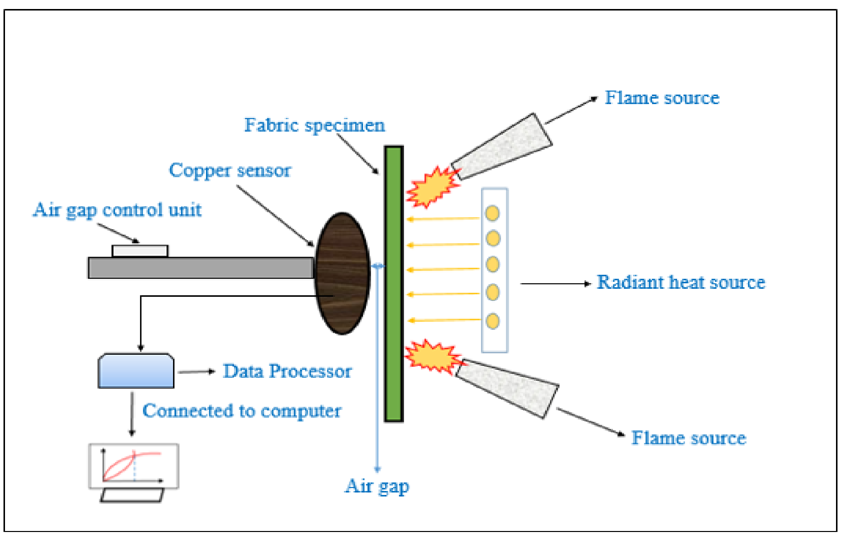

Figure 2. Schematic representation of the main components of vertical radiant and flame protective performance tester

A J-type thermocouple was used and welded at the centre of the copper disk. The sensor acts as a transducer that converts heat energy to electric current proportional to the Q incident on it. The test specimen is flanked tightly with the help of a metal gripper having the outside dimensions of 15 cm (L) x 15 cm (W) each and a central open space of 10 cm x 10 cm. The output signal emitted from the RTD sensor is captured by a Data Acquisition System, and analyzed with ADAM 4015 processer. The output data was scanned at the rate of one hundred scans every second and accumulated in the memory of the computer by the software. A series of electrically operated quartz lamps mounted on a metallic stationary block generate radiant heat energy. The electrical power supply is connected to the lamps' input terminal via a variable resistance, which acts as an input voltage regulator and keeps the radiant heat intensity at a desired level. The calorimeter is mounted on a movable insulation board installed in compliance with ISO 9151. The air gap D between the sensor and fabric is adjusted by placing the movable assembly at the chosen distance. The temperature rise was recorded by the J-type thermocouple. The temporal variation of temperature was recorded to determine tolerance time ‘t’ on plotting with the Stoll curve as shown in Figure 3. Calibration has been performed for the sensor used in the experimental setup. As the experimental setup used in the present study used the copper calorimeter to measure the temperature rise with time, it was also calibrated. To check the validity of copper calorimeter readings, its readings were compared with an IR-gun reading. For this, the exposed copper disk surface of the copper calorimeter sensor was subjected to flame for some duration and left open in the atmosphere to cool it down. During this cooling period of the sensor, the temperature was recorded with the copper calorimeter sensor and an IR gun focusing on the exposed surface of the copper disk. Good agreement was observed between the two measurements with a maximum difference of approximately 3.5 ^{o}C.

The empirical equation relating to cumulative heat (G) and time (Stoll curve) is given by:

$$G = (5.0204)*t^{0.2809} \quad (1)$$

The value of H was calculated using the equation:

$$\text{Heat flux} = \frac{Q * c * \Delta T}{A * \Delta t} \quad (2)$$

Where, Q = Copper calorimeter’s mass (kg), c = Copper’s specific heat (J/kg.K), ΔT = (Final temperature-starting temperature) (Kelvin), A= Copper calorimeter's surface area (m^2), Δt = (Final time – starting time)

The absorptivity of black paint applied on a copper calorimeter is assumed to be 0.90 in the above relationship.

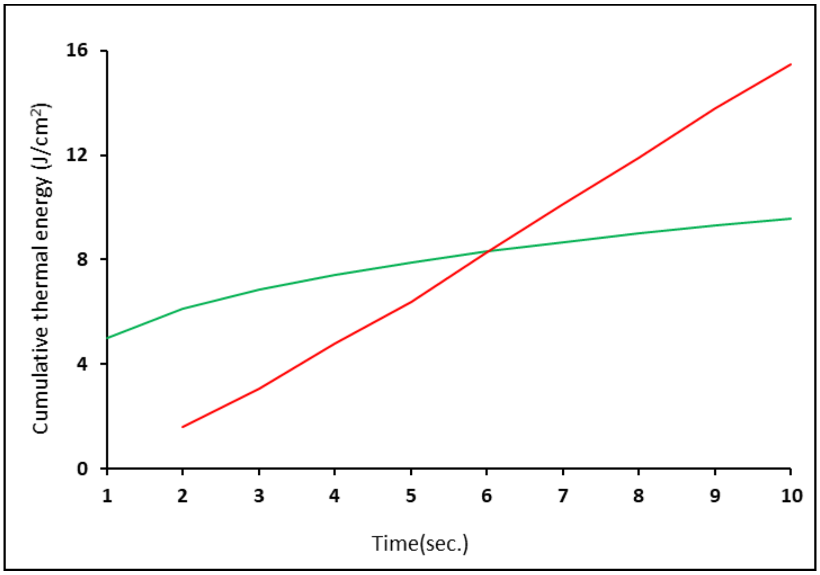

Figure 3. Run 8 of radiant exposure Stoll criterion curve (Green colour) and experimental plot (Red colour) using cumulative heat

The protection time was computed using the abscissa value at the junction of two curves, which represents the clothing's second-degree burn time. A longer second-degree burn duration suggests stronger fire resistance and heat resistance. The time it takes for total heat energy to induce harm on the opposite side of a fabric is measured. The term D refers to the distance between the fabric and the copper calorimeter's sensor.

Design of Experiment

The basic layout of the design created for the quantification of output response obtained against each level of the independent variable was conducted by adopting the Box-Behnken design of experiments (DOE). The independent variables included (a) pick density of test fabric in weft direction (P) at three levels, namely, 40, 52 and 64 PPI, (b) Q corresponding to 0.5,1 and 1.5 cal/cm^2/sec (c) D between sensor and fabric also at three levels of 0, 12.5 and 25 mm. Multiple regression analysis of the experimental data was carried out by using the software Design Expert® version 11 for the computation of the empirical relation between independent variables and output responses measured by recording the values of protection time.

RESULTS AND DISCUSSIONS

Physical Properties

The physical properties of fabrics with different densities are tabulated in Table 3. The areal density of fabrics increases with an increase in picks per inch owing to the inclusion of more yarns per unit length. Since the compactness of structure in denser fabrics is greater, the cover factor also increases with an increase in pick density. The data showing trend lines of change in thickness and bulk density lack consistency. The air permeability of fabrics is inversely related to areal density and so decreases in the reverse order.

Table 1. Description of physical properties of fabrics for the outer layer

S.No.	Fabric structure	Ends per inch	Picks per inch	Areal Density (g/m^2)	Thickness (mm)	Air Permeability ($cm^3/s/cm^2$)	Cover Factor
1	Honeycomb	42	40	117.6	0.523	112.32	15.3
2	Honeycomb	42	52	126.7	0.535	82.34	17.2
3	Honeycomb	42	64	143.6	0.541	55.72	19.4

Box-Behnken DOE

Pick density, heat flux, and air gap between fabric and copper calorimeter are all elements that affect fire protection effectiveness. The interaction of these three parameters impacts the performance of the end product. The current study examined the impact of varying two independent factors on fire-protective clothing performance by measuring protection time. A surface response curve was made using the corresponding values of protection time, with the values of the independent variables shown on the x-axis and y-axis. Also included in this empirical model are equations relating process parameters to outputs. Table 2 lists the levels and process parameters for the Box-Behnken DOE.

Table 2. Three Process parameters and levels of Box-Behnken DOE

Factor	Name	Units	Level			Mean	SD
			Low	Medium	High		
A	Pick density	picks per inch	40 (-1)	52 (0)	64 (+1)	52	9
B	Heat flux	$cal/cm^2/sec$	0.5 (-1)	1 (0)	1.5 (+1)	1	0.365
C	Air gap	mm	0 (-1)	12.5 (0)	25 (+1)	12.5	9.129

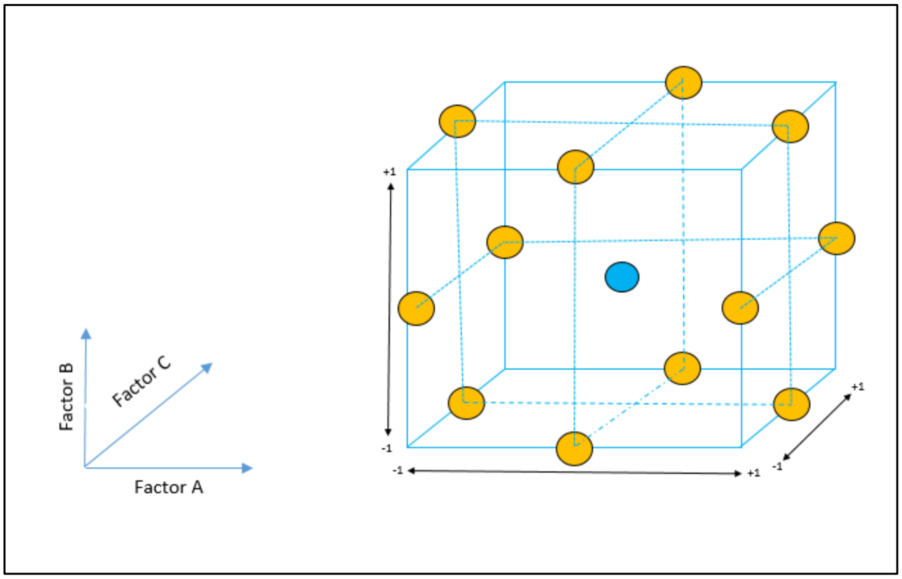

Figure 4. The geometry of Box-Behnken design with the location of middle points of edges and centre points

The geometry of the Box-Behnken design with the location of the middle points of edges and centre points is shown in Figure 4. Box-Behnken design identifies a lack of fit, and use of blocks and allows for the interpretation of quadratic model. Srinivasan et al. identified the variables that are used for the design are located within similarly spaced intervals [44]. The relations between the number of experimental points and the number of coefficients are reasonable. Koushua et al. and Ferreira et al. opined that the Box-Behnken DOE was more efficient compared to the three-level full factorial design and central composite design [42,43]. Srinu Babu et al. found that DOE was capable of offsetting the drawbacks of the one-variable-at-a-time method [40]. The authors suggested using a three-level, three-factor Box-Behnken design to create empirical model equations that correlate output responses to process parameters. As a result of these results, the Box-Behnken design was chosen as the best statistical tool for optimizing process parameters at three distinct levels high (+1), medium (0), and low (-1) to obtain the optimum R_T and F_T. Table 3 represents the 15 experiment runs' raw data and coded values.

Table 3. Actual values and coded values for output response

Run	Pick density (P)	Heat Flux (Q)	Air Gap (D)	Output response of radiant protection time (sec.)	Output Response of flame protection time (sec.)
1	52 (0)	1.5 (+1)	25 (+1)	6.4	6.9
2	52 (0)	1(0)	12.5 (0)	6.9	8.5
3	52 (0)	1 (0)	12.5 (0)	6.9	7.6

https://doi.org/10.31881/TLR.2023.213

Run	Pick density (P)	Heat Flux (Q)	Air Gap (D)	Output response of radiant protection time (sec.)	Output Response of flame protection time (sec.)
4	40 (-1)	1 (0)	0 (-1)	6.8	6.9
5	40 (-1)	1 (0)	25 (+1)	7.5	8.6
6	64 (+1)	0.5 (-1)	12.5 (0)	18.4	18.6
7	64 (+1)	1 (0)	0 (-1)	5.1	6.8
8	40 (-1)	1.5 (+1)	12.5 (0)	5.8	7.2
9	52 (0)	1 (0)	12.5 (0)	6.9	8.1
10	52 (0)	0.5 (-1)	0 (-1)	16.1	16.3
11	64 (+1)	1 (0)	25 (+1)	7.8	8.6
12	52 (0)	0.5 (-1)	25 (+1)	17.4	17.5
13	52 (0)	1.5 (+1)	0 (-1)	5.8	6.9
14	40 (-1)	0.5 (-1)	12.5 (0)	17.2	17.7
15	64 (+1)	1.5 (+1)	12.5 (0)	5.5	6.8

Statistical Analysis

The Model F-value of the Box-Behnken design is 32.06 for radiant and 24.94 for flame, suggesting that the model is significant. The p-value for the model is 0.0007 and 0.0012 for radiant and flame exposure respectively. All the terms are significant because the values of p are less than 0.05. In this case all types of parameters (viz., single process parameters P, Q and D, interaction parameters P *Q, P*D and Q*D and square of parameters P^2, Q^2 and D^2 are significant terms in this experimental design. Design Expert ® version 11 was used to fit the experimental response data into a polynomial equation of the second degree.

The computed values of protection time to the process parameters may be expressed by the empirical equations 1 and 2 are shown below:

$$'R_t'=+13.53102+0.33831*P-22.84167*Q+0.24133*D-0.14167*P*Q-0.0015*P*D-0.044*Q*D-0.0011*P^2+10.36667*Q^2-0.0041*D^2 \quad (3)$$

$$'F_t'=+9.36435+0.50914*P-22.29167*Q+0.31733*D-0.12917*P*Q-0.002*P*D-0.072*Q*D-0.0029*P^2+9.91667*Q^2-0.0048*D^2 \quad (4)$$

Where, P = Pick density, Q = Heat Flux and D = Air Gap

Notably, first and second-order coefficients effectively describe the process whereas higher-order coefficients are insignificant. Regression analysis was used to relate the prediction to the experimental results. The correlation coefficient between the predicted protection time and actual protection time is high (R^2 = 0.985 for radiant and 0.978 for flame) as shown in Figure 5. Signal to noise ratio was measured by "Adeq Precision". The value of the signal-to-noise ratio is 16.43 for radiant and 14.25 for flame, implying that this Box-Behnken design is sufficiently strong in comparison to the minimum desirable ratio of greater than 4. Hence, this model may be used as a guide to help narrow down the design options.

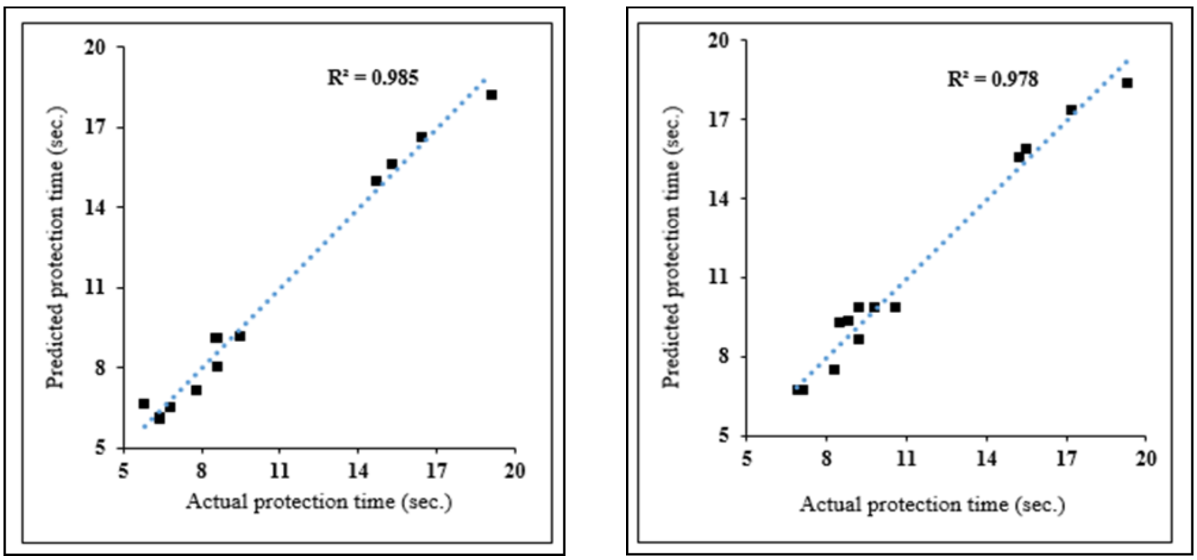

a) b)

Figure 5. Predicted protection time vs. Actual (Real) protection time of a) Radiant and b) Flame exposure

Effect of Pick density and heat flux at a constant level of air gap on protection time

The 3D surface response plot depicted in Figure 6 describes the effect of pick density P and heat flux Q on radiant protection time (R_T) and flame protection time (F_T) at a middle level of air space D. The 3D surface response curve for both exposures is showing very less difference. More objective information was gathered by substituting the three-level values of all three parameters in equation (3) for radiant exposure and in equation (4) for flame exposure. The interactive terms with very low coefficients were neglected. Figures 7 (A) and 7 (B) show the calculated protection time for radiant and flame exposures, respectively.

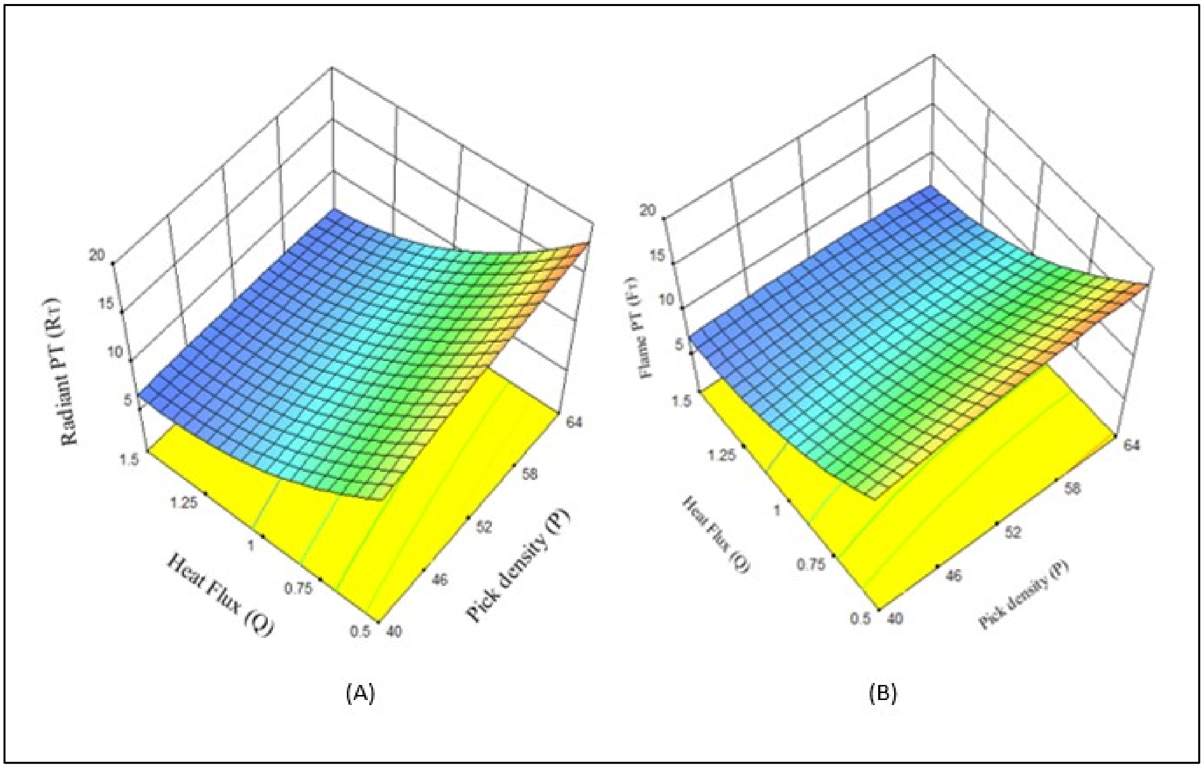

Figure 5. The output response of Radiant (a) and Flame (b) protection time with input process variables of pick density and heat flux at a constant air gap of 12.5 mm

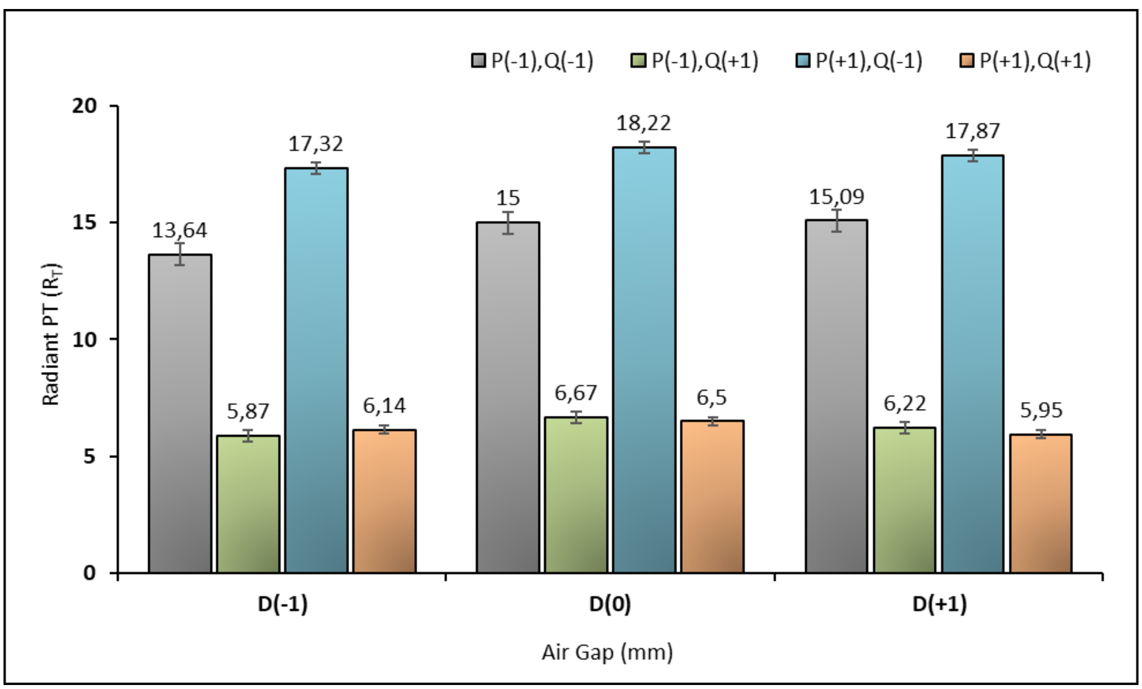

a)

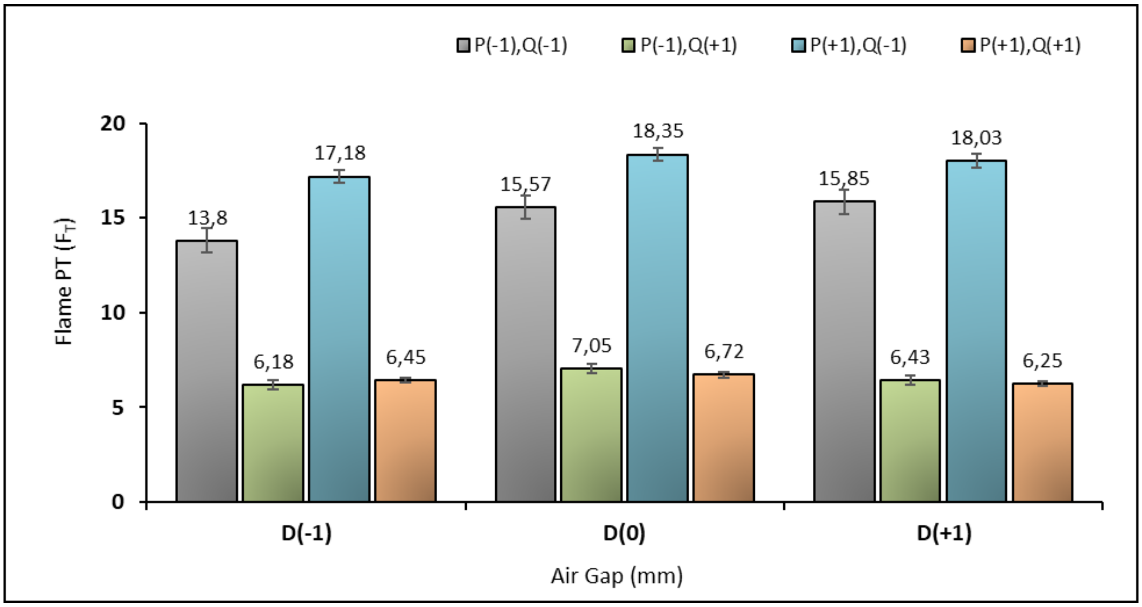

b)

Figure 7. Effect of increasing air gap width between the fabric and copper sensor on radiant (a) and flame (b) exposure on a protection time

The values of protection time obtained against a given set of values for P and Q were found to improve with an increase in D from D (-1) to D (0) but not much change is observed from D (0) to D (+1) in both exposure for high level of heat flux and high level of heat intensity due to the impact of high heat flux and pick density (Figure 7). A logical explanation for this behaviour is the fact that the heat flux incident on the sensor diminishes by a factor of $1/D^2$ for an increase in air gap. In other words, doubling D would reduce Q by one-fourth of its original intensity and a proportionate rise in protection time. For the pair of isothermal coordinates Q (+1), P (-1) and Q (+1), P (+1) the gain in protection time was appreciably low (4.6% for radiant and 4.3% for flame) than that for the pair of coordinates Q (-1), P (-1) and Q (-1), P (+1) (26.9% for radiant and 24.5% for flame) at the lower level of air gap. Here, the pick density of fabric is more effective in controlling the protection time at the low level of heat intensity.

The protection time stood at its lowest value is 5.87 for radiant exposure with the set of process parameters defined by Q (+1), P (-1) and D (-1) and 6.18 for flame exposure at same coordinates Q (+1), P (-1) and D (-1) while the best performance or highest protection time was realized at Q (-1), P (+1) and D (0), which are 18.22 and 18.35 for radiant and flame exposure respectively. The increase in protection time from D(-1) to D(0) was 9.9% for radiant and 12.8% for a flame for parameters of P(-1), Q(-1); 13.6% for radiant and 14% for a flame for parameters of P(-1), Q(+1); 5.19% for radiant and 6.8% for a flame for parameters of P(+1), Q(-1) and 5.86% for radiant and 4.18% for a flame for parameters of P(+1), Q(+1) due to present of a barrier in form of air but not same trend obtained from 12.5 to 25 mm air gap (i.e. 0.6 % for P(-1), Q(-1); -1.9% for P(+1), Q(-1) etc.). The reduction in radiant and flame protection time is 56.9% and 55.2% respectively for P (-1), Q (-1) to Q (+1) but 64.5% and 62.4% respectively for P (+1), Q (-1) to Q (+1) which is approximately 7-7.5 % less compared to P (+1), Q (-1)-to Q (+1) due to the more yarn burns in case of high pick density. The improvement in radiation and flame protection time is 26.9% and 24.5% respectively for Q (-1) and P (-1) to P (+1), and approx. 4.5% in both exposure for Q (+1) and P (-1) to P (+1), at a constant level of air gap D (-1) attributed to fabric density alone since Q and D are constant and P is the only variable. The fire-protective fabric lies between the source of heat and the sensor and acts as a barrier in the path of transmission of heat; the increase in pick density results in higher thread count per unit area and lower air permeability (Table 1). At higher pick density, all these factors offer concerted resistance to the transmission of heat by radiation and flame. As a result, the efficiency of the thermal insulation property improves which manifests itself by boosting the protection time. The maximum improvement in protection time is obtained for P (+1), Q (-1) to Q (+1) at D (+1) in the analysis of the effect of air gap as shown in figure 7.

Effect of the air gap and pick density at a constant level of heat flux on protection time

The surface response graph shown in Figure 8 and twenty-four values computed of protection time in this exercise are graphically presented in Figure 9, which represents the response on radiant and flame protection time for P (-1, 0, +1) vs D (-1, 0, +1) at a given level of Q. Figure 9 indicate that the quantity decreases remarkably in the direction Q (-1) to Q (0) to Q (0) to Q (+1).

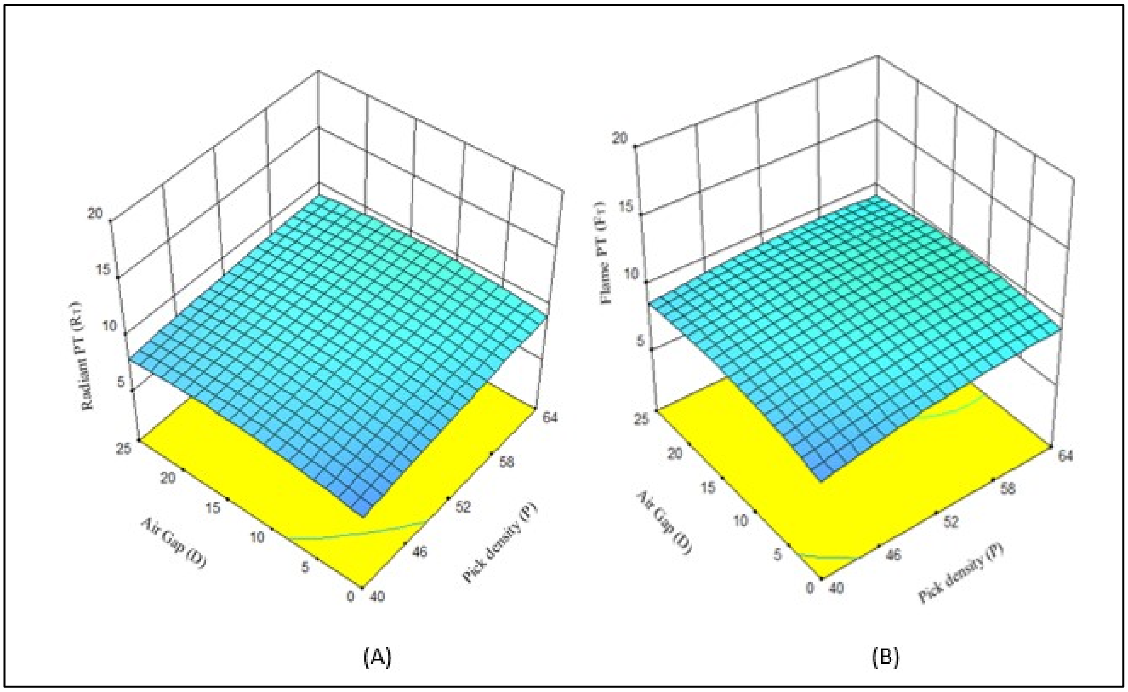

Figure 6. The output response of Radiant (a) and Flame (b) protection time with input process variables of the air gap and pick density at a heat flux of 1 cal/cm^2/sec

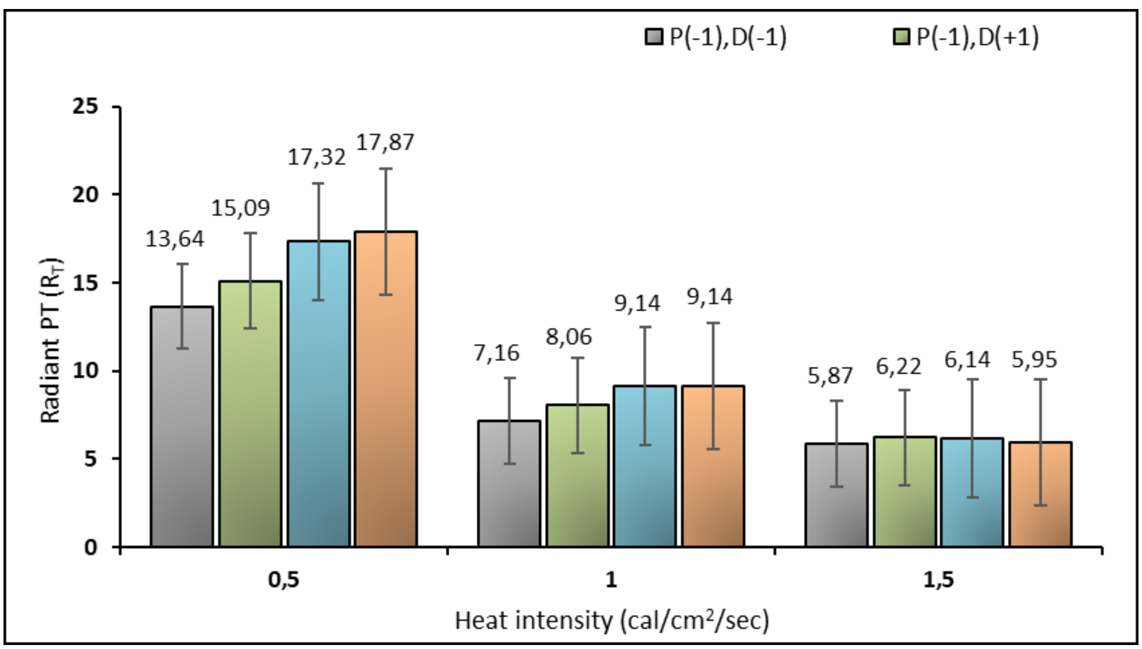

a)

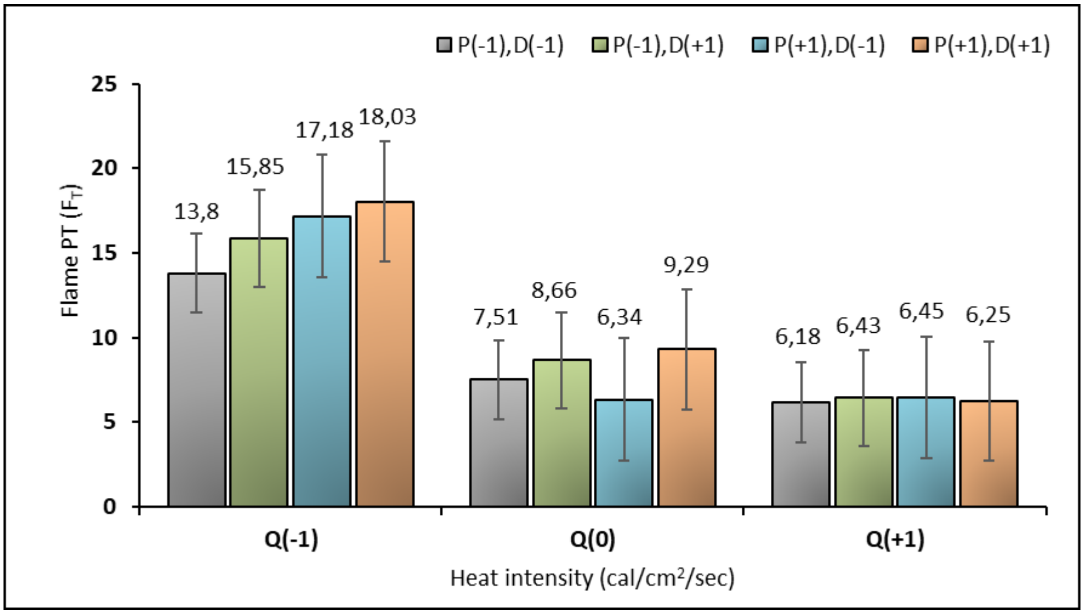

b)

Figure 9. Effect of increasing heat flux on radiant a) and flame b) protection time

The Gross loss from Q(-1) to Q(+1) in protection time from 55-56% for P(-1),D(-1) to 68-69% for P(+1),D(+1) . At a lower level of pick density P (-1) if we increase the air gap from D(-1) to D(+1) then the radiant and flame protection time increase by 10.63% and 14.85% respectively for Q(-1),12.6% and 15.32% respectively for Q(0) and 5.96% and 4% respectively for Q(+1). The role of the air gap in improving the protection time values has already been explained. The maximum gain for radiant is 27.6% occur at Q(0), D(-1) and P(-1) to P(+1) and 46 % for flame occur at Q(0),P(+1),D(-1) to D(+1). The maximum improvement in protection time is obtained for D (-1), P (-1) to P (+1) at Q (-1) in the analysis of the effect of heat flux, as shown in Figure 9.

Effect of the air gap and heat flux at a constant level of pick density on protection time

The dependence of protection time on the process parameters Q and D at different levels of P is shown in Figure 10. Subsequent work up on equations 3 and 4 according to the above description afforded another set of twenty-four values of protection time against each combination of D and Q at different levels of pick density.

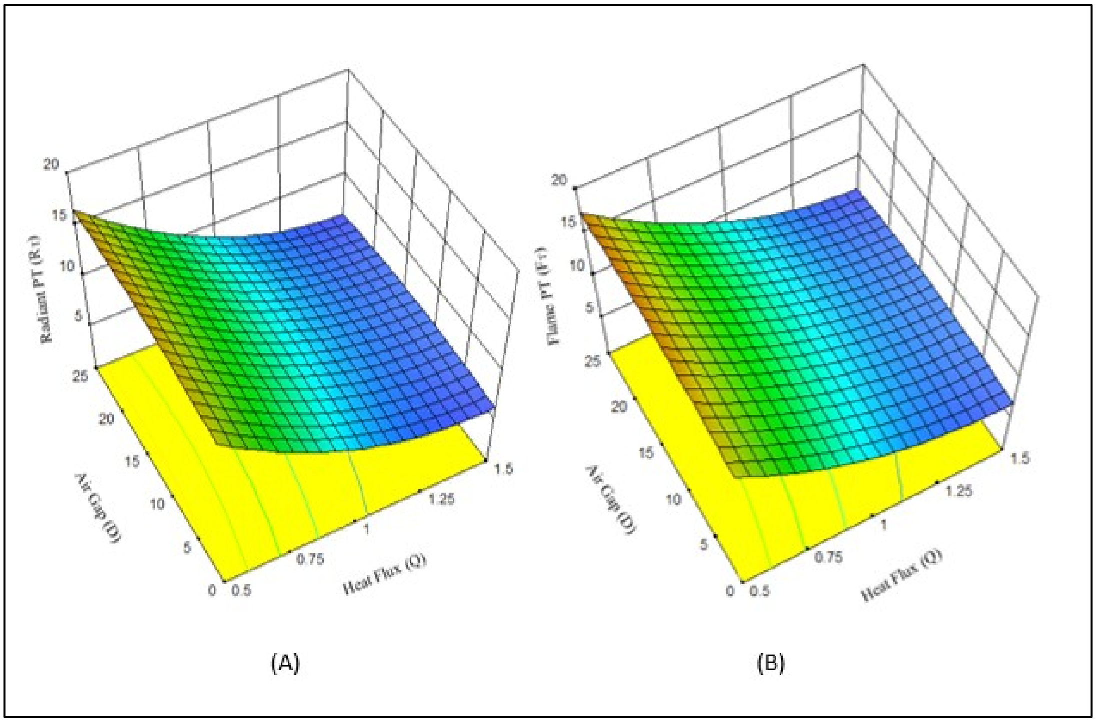

Figure 7. Output response of Radiant (a) and Flame (b) protection time with input process variables of heat flux and air gap at pick density of 52 picks per inch

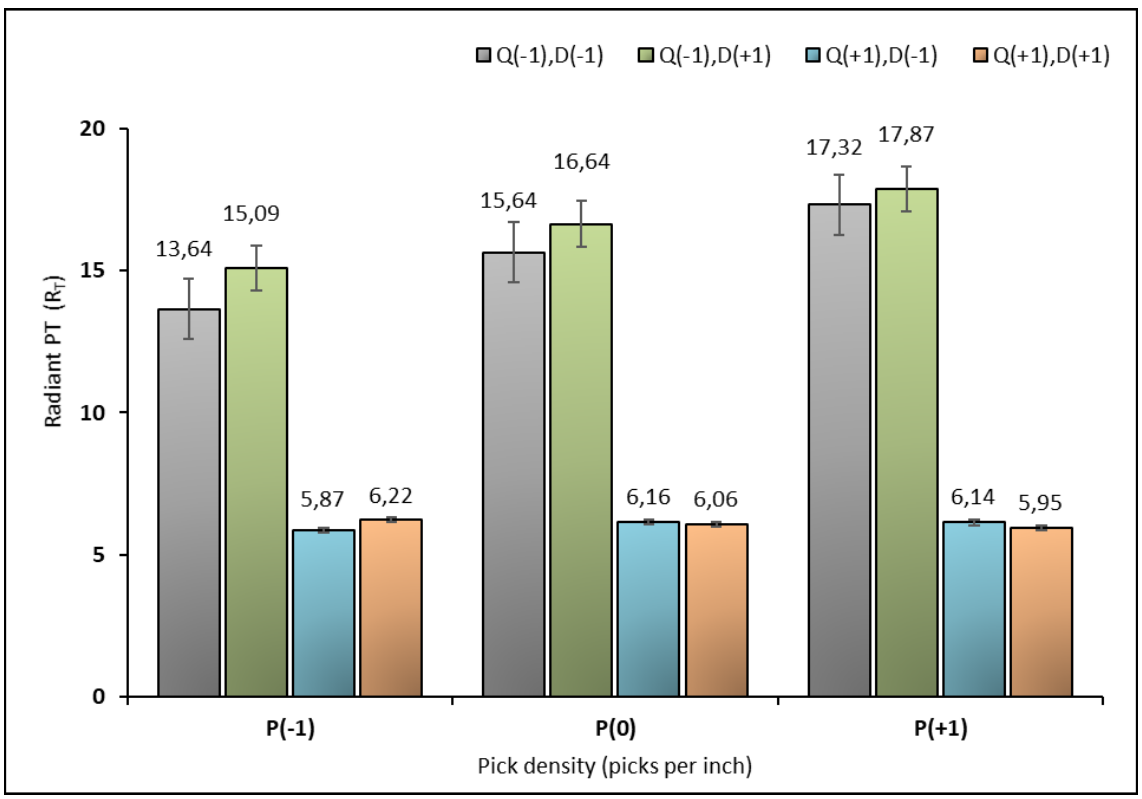

a)

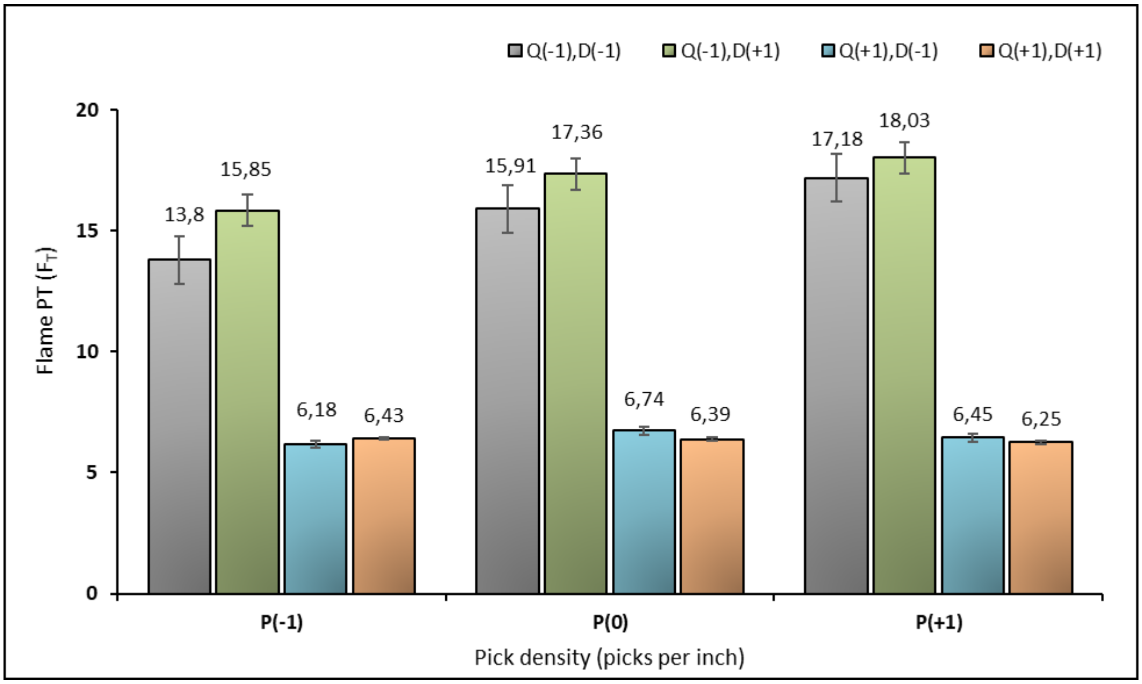

b)

Figure 11. Effect of increasing pick density on radiant a) and flame b) protection time

The results are depicted in Figure 11. At a lower level of heat flux and air gap Q (-1), D (-1) the improvement in protection time is 14.7% for the radiant and 15.2% for the flame from P (-1) to P (0), 10.7% for radiant and 8% for the flame from P (0) to P (+1). The overall improvement in protection time is 27% for radiant and 24.5% for flame for the same coordinates. At a higher level of heat flux if we increase the level of air gap and pick density then not much less improvement is observed in protection time.

Here, exposure to different combinations of Q and D less affects the values of protection time. This suggests that the D is not a determining factor in such an occasion. At constant pick density if we increase the air gap from D(-1) to D(+1) the improvement in protection time is 10.63% for radiant and 14.85% for flame at the lower level of heat flux but 5.96% for radiant and 4% for flame at high level of heat flux. The reduction in protection time occurs due to an increase in the level of heat flux and the maximum reduction occurs at P (+1), D (+1) and Q (-1) to Q (+1). In the analysis of the effect of pick density, the highest improvement in protection time is achieved at D (+1), Q (-1) to Q (+1), at P (-1), as shown in Figure 11. The combined effect of all three process parameters of pick density, heat flux and air gap from a lower level to a higher level on protection time is explained with the help of coordinates of the cubic figure shown in Figure 12.

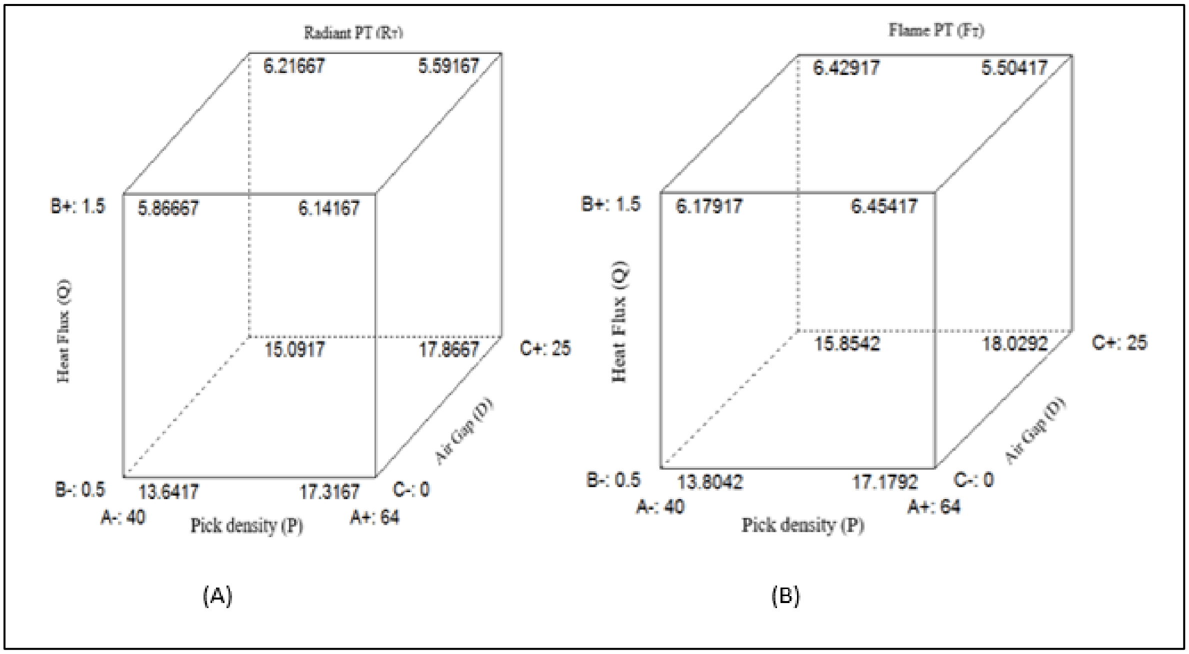

Figure 8. Effect of the air gap, Heat flux and pick density on Radiant (a) and Flame (b) protection time

This research is useful in determining the relationship between the protection time during radiant heat flame exposure and the processing parameters. Based on the end applications (outer layer of fire protective clothing and single layer station wear uniform), the required protective performance (Low, medium and semi-high level of heat flux) of the outer layer may be created. Fire protective clothing, which is commonly recommended for protective applications, is made with an outer layer that has a longer protection period. The pick density of the outer layer has a significant impact on mechanical qualities such as tear, tensile, and seam properties. Depending on the ultimate use, such as radiant heat or flame, the optimal quantity of picks per inch and air gap is necessary. It looked at all three process parameters at three levels for both exposures (radiant heat and flame) in one paper and used an empirical equation for each one. Researchers will also be able to figure out how to get values in a certain range of a process parameter by doing a single calculation. They will also be able to figure out how to explore the empirical equation of the Box-Behnken model and other surface response curves.

CONCLUSION

This study optimized the protective effectiveness of the outer shell honeycomb woven fabric of fire-resistant apparel made using Nomex IIIA yarns. The process parameters evaluated for the evaluation include pick density (P), heat flux (Q), and air gap (D) under flame and radiant exposure, with Box-Behnken DOE used as a statistical tool. To forecast the values of radiant and flame protection time, two empirical equations were created, and linear and interaction effects of P vs. Q, P vs. D, and Q vs. D were calculated. The experimental and predicted values of protection time have a strong correlation coefficient (R^2 = 0.985 for radiant and 0.978 for flame). The lowest protection time was 5.87 for radiant exposure and 6.18 for flame exposure with the following process parameters: heat flux of 1.5 cal/cm^2/sec, air gap of 0 mm, and pick density of 40 picks per inch. The highest protection time was 18.22 for radiant and 18.35 for flame exposure with the following process parameters: heat flux of 0.5 cal/cm^2/sec, an air gap of 12.5 mm, and pick density of 64 picks per inch. All other values for protection time come between these two extremes. The maximum improvement in protection was obtained at a high level of air gap (25 mm), low level of heat flux (0.5 cal/cm^2/sec) and low level of pick density (40 picks per inch). Presented research and obtained results will help the researchers obtain values of protection time in the designated range of process parameters by a single calculation and explore the empirical equation of the Box-Behnken model as well as other surface response curves.

Author Contributions

Conceptualization – Rathour R and Maurya S; methodology – Rathour R and Das T; formal analysis – Rathour R and Maurya S and Das T; investigation – Rathour R, Das A and Alagirusamy R; resources – Das A and Alagirusamy R; writing-original draft preparation – Rathour R, Rajput B and Alagirusamy R; writing-review and editing – Rathour R, Rajput B and Das A; visualization – Rathour R and Maurya S and Das T; supervision – Rajput B, Das A and Alagirusamy R. All authors have read and agreed to the published version

Conflicts of Interest

The authors declare no conflict of interest.

Funding

This research received no external funding.

Acknowledgements

This work is part of the completed project "Design and Development of Extreme Heat Protective Clothing for Defense Application" (Project code – SITEX 05 / RP03456, Funded by Joint Advanced Research Centre, an initiative by IIT Delhi and Defence Research and Development Organization, Ministry of Defence, Govt. of India).

REFERENCES

[1] Chakraborty S, Kothari V. Effect of Moisture and Water on Thermal Protective Performance of Multilayered Fabric Assemblies for Firefighters. Indian Journal of Fibre & Textile Research. 2017; 42(1):94–99.

[2] Meredith M, Den Hartog E, Barker R, Ross K. A review of garment ventilation strategies for structural firefighter protective clothing. Textile Research Journal. 2016; 86(7):727–742. https://doi.org/10.1177/0040517515595029

[3] Rathour R, Rajput B, Das A, Alagirusamy R. Performance analysis of shell fabric of fire protective clothing for different process parameters. The Journal of The Textile Institute. 2022; 2022:1–10. https://doi.org/10.1080/00405000.2022.2145441

[4] Rajput B, Mahesh N, Rathour R, Das T, Ray B, Das A, et al. Performance analysis of multilayer flame-retardant fabric ensembles for different exposure conditions using numerical modeling. The Journal of The Textile Institute. 2022; 115(2):218-227. https://doi.org/10.1080/00405000.2022.2156717

[5] Rathour R, Krishnasamy J, Das A, Alagirusamy R. Water vapor transmission and electromagnetic shielding characteristics of stainless steel/viscose blended yarn woven fabrics. Journal of Industrial Textiles. 2023; 53:152808372211492. https://doi.org/10.1177/15280837221149217

[6] Udayraj, Talukdar P, Das A, Alagirusamy R. Heat and mass transfer through thermal protective clothing - A review. International Journal of Thermal Sciences. 2016; 106:32–56. https://doi.org/10.1016/j.ijthermalsci.2016.03.006

[7] Zhang Z, Ni J, Zhou Y. The Effect of Arm Postures and Garment Style on Local Mobility and Thermal Insulation. AATCC Journal of Research. 2022; 9(1):12–22. https://doi.org/10.1177/23305517211060813

[8] Subham, Rathour R, Das A, Alagirusamy R. Development of thermal liner for extreme heat protective clothing using aerogel technology. Journal of the Textile Institute. 2023. https://doi.org/10.1080/00405000.2023.2201913

[9] Maurya H, Rathour R, Udayraj, Das A, Alagirusamy R. Mathematical modelling and experimental validation of thermal conductivity of outer layer of fire protective clothing. Journal of the Textile Institute. 2023. https://doi.org/10.1080/00405000.2023.2284035

[10] Hasan Z. Impact of Woven Fabric Structure and Material on Thermo-physiological Comfort Properties of Cut Protective Textile. Annual Technical Volume. Textile Engineering Division Board. p. 9–16.

[11] Shaid A, Wang LPR. Textiles for Firefighting Protective Clothing. In: Song G, Wang F, editors. Firefighters' Clothing and Equipment: Performance, Protection, and Comfort. CRC Press; 2018.

[12] Hristian L, Bordeianu DL, Iurea P, Sandu I, Earar K. Study of the tensile properties of materials destined to manufacture protective clothing for firemen. Materiale Plastice. 2014; 51(4):405–409.

[13] Gao H, Deaton AS, Fang X, Barker RL, DenHartog E, Watson K. Effects of Outer Shell Fabric Color, Smoke Contamination, and Washing on Heat Loss through Turnout Suit Systems. Textile Research Journal. 2022; 92(11–12):1909–1922. https://doi.org/10.1177/00405175211073353

[14] Rathour R, Das A, Alagirusamy R. Impact of repeated radiative heat exposure on protective performance of firefighter's protective clothing. Journal of Industrial Textiles. 2022; 52:1–30. https://doi.org/10.1177/15280837221117610

[15] Shaker K, Umair M, Jabbar M, Baitab DM, Nawab Y, Afzal A, et al. Effect of fabric structural design on the thermal properties of woven fabrics. Thermal Science. 2018; 2018:3059–3066. https://doi.org/10.2298/TSCI170707003S

[16] Nazir MU, Javaid MU, Shaker K, Nawab Y, Hussain T, Umair M. Effect of picking sequence on thermo-physiological comfort of bilayer woven fabrics. Research Journal of Textile and Apparel. 2023; 27(4):530-542. https://doi.org/10.1108/RJTA-10-2021-0120

[17] Lei Z. Review of the study of relation between the thermal protection performance and the thermal comfort performance of firefighters' clothing. Journal of Engineered Fibers and Fabrics. 2022; 17. https://doi.org/10.1177/15589250211068032

[18] Wakatsuki K, Seita R, Watanabe N, Muramoto S, Kobayashi Y, Morikawa H. Characterization of Air Gaps and Their Impact on the Thermal Insulation Performance of Multi-layer Firefighter Clothing. Fire Technology. 2022; 58:1863-1887. https://doi.org/10.1007/s10694-022-01222-5

[19] Shalev I, Barker RL. Analysis of Heat Transfer Characteristits of Fabrics in an Open Flame Exposure. Textile Research Journal. 1983; 53(8):475–482. https://doi.org/10.1177/004051758305300806

[20] Das A, Alagirusamy R, Kumar P. Study of heat transfer through multilayer clothing assemblies: A theoretical prediction. Autex Research Journal. 2011; 11(2):54–60. https://doi.org/10.1515/aut-2011-110205

[21] Sun G, Yoo HS, Zhang XS, Pan N. Radiant Protective and Transport Properties of Fabrics Used by Wildland Firefighters. Textile Research Journal. 2000; 70(7):567–573. https://doi.org/10.1177/004051750007000702

[22] Kutlu B, Cireli A. Thermal analysis and performance properties of thermal protective clothing. Fibres and Textiles in Eastern Europe. 2005; 13(3):58–62.

[23] Rathour R, Das A, Alagirusamy R. Study on the influence of constructional parameters on performance of outer layer of thermal protective clothing. The Journal of The Textile Institute. 2022; 51(5_suppl):8107S-8126S. https://doi.org/10.1177/15280837211054582

[24] Udayraj, Talukdar P, Das A, Alagirusamy R. Effect of structural parameters on thermal protective performance and comfort characteristic of fabrics. Journal of the Textile Institute. 2017; 108(8):1430–1441. https://doi.org/10.1080/00405000.2016.1255123

[25] Lee YM, Barker RL. Thermal protective performance of heat-resistant fabrics in various high-intensity heat exposures. Textile Research Journal. 1987; 57(3):123–132. https://doi.org/10.1177/004051758705700301

[26] Mandal S, Song G, Ackerman M, Paskaluk S, Gholamreza F. Characterization of textile fabrics under various thermal exposures. Textile Research Journal. 2013; 83(10):1005–1019. https://doi.org/10.1177/0040517512461707

[27] Song G, Paskaluk S, Sati R, Crown EM, Dale JD, Ackerman M. Thermal protective performance of protective clothing used for low radiant heat protection 2011; 81(3):311-323. https://doi.org/10.1177/0040517510380108

[28] Fu M, Weng WG, Yuan HY. Quantitative assessment of the relationship between radiant heat exposure and protective performance of multilayer thermal protective clothing during dry and wet conditions. Journal of Hazardous Materials. 2014; 276:383–392. https://doi.org/10.1016/j.jhazmat.2014.05.056

[29] Udayraj, Talukdar P, Alagirusamy R, Das A. Heat transfer analysis and second degree burn prediction in human skin exposed to flame and radiant heat using dual phase lag phenomenon. International Journal of Heat and Mass Transfer. 2014; 78:1068–1079. https://doi.org/10.1016/j.ijheatmasstransfer.2014.07.073

[30] Sawcyn CMJ, Torvi DA. Improving Heat Transfer Models of Air Gaps in Bench Top Tests of Thermal Protective Fabrics. Textile Research Journal. 2009; 79(7):632–644. https://doi.org/10.1177/0040517508093415

[31] Talukdar P, Torvi DA, Simonson CJ, Sawcyn CMJ. Coupled CFD and radiation simulation of air gaps in bench top protective fabric tests. International Journal of Heat and Mass Transfer. 2010; 53(1–3):526–539. https://doi.org/10.1016/j.ijheatmasstransfer.2009.04.041

[32] Song G, Ding D, Chitrphiromsri P. Numerical simulations of heat and moisture transport in thermal protective clothing under flash fire conditions. International Journal of Occupational Safety and Ergonomics. 2008; 14(1):89–106. https://doi.org/10.1080/10803548.2008.11076752

[33] Torvi DA, Threlfall TG. Heat transfer model of flame resistant fabrics during cooling after exposure to fire. Fire Technology. 2006; 42(1):27–48. https://doi.org/10.1007/s10694-005-3733-8

[34] Lu Y, Li J, Li X, Song G. The effect of air gaps in moist protective clothing on protection from heat and flame. Journal of Fire Sciences. 2013; 31(2):99–111. https://doi.org/10.1177/073490411245734

[35] Fu M, Weng W, Yuan H. Effects of multiple air gaps on the thermal performance of firefighter protective clothing under low-level heat exposure. Textile Research Journal. 2014; 84(9):968–978. https://doi.org/10.1177/0040517513512403

[36] Yu Z, Liu J, He H, Ma S, Yao J. Flame-retardant PNIPAAm/sodium alginate/polyvinyl alcohol hydrogels used for fire-fighting application: Preparation and characteristic evaluations. Carbohydrate Polymers. 2021; 255:117485. https://doi.org/10.1016/j.carbpol.2020.117485

[37] He H, Liu J, Wang Y, Zhao Y, Qin Y, Zhu Z, et al. An Ultralight Self-Powered Fire Alarm e-Textile Based on Conductive Aerogel Fiber with Repeatable Temperature Monitoring Performance Used in Firefighting Clothing. ACS Nano. 2022; 16(2):2953–2967. https://doi.org/10.1021/acsnano.1c10144

[38] Rathour R, Das A, Alagirusamy R. Studies on the influence of process parameters on the protection performance of the outer layer of fire-protective clothing. Journal of Industrial Textiles. 2022; 51(5_suppl):8107S-8126S. https://doi.org/10.1177/15280837211054582

[39] Ba-Abbad MM, Chai PV, Takriff MS, Benamor A, Mohammad AW. Optimization of nickel oxide nanoparticle synthesis through the sol-gel method using Box-Behnken design. Materials and Design. 2015; 86:948–956. https://doi.org/10.1016/j.matdes.2015.07.176

[40] Srinu Babu G, Shiva Kiran RR, Lokeswari N, Jaya Raju K. Optimization of protease production from Aspergillus oryzae sp. using Box-Behnken experimental design. E-Journal of Chemistry. 2007; 4(2):145–153. https://doi.org/10.1155/2007/254613

[41] Maurya S, Rathour R, Mishra P, Mishra D, Das A, Ramasamy A. Studies on the effect of process parameters on the thermal protective performance of multilayer thermal protective clothing. Journal of the Textile Institute. 2023. https://doi.org/10.1080/00405000.2023.2250486

[42] Kousha M, Daneshvar E, Dopeikar H, Taghavi D, Bhatnagar A. Box-Behnken design optimization of Acid Black 1 dye biosorption by different brown macroalgae. Chemical Engineering Journal. 2012; 179:158–168. https://doi.org/10.1016/j.cej.2011.10.073

[43] Ferreira SLC, Bruns RE, Ferreira HS, Matos GD, David JM, Brandão GC, et al. Box-Behnken design: An alternative for the optimization of analytical methods. Analytica Chimica Acta. 2007; 597(2):179–186. https://doi.org/10.1016/j.aca.2007.07.011

[44] Srinivasan T, Palanikumar K, Rajagopal K, Latha B. Optimization of delamination factor in drilling GFR–polypropylene composites. Materials and Manufacturing Processes. 2017; 32(2):226–233. https://doi.org/10.1080/10426914.2016.1151038

[45] Das T, Das A, Alagirusamy R. Study on thermal protective performance of thermal liner in a multi-layer clothing under radiant heat exposure. Journal of Industrial Textiles. 2022; 51(5_suppl):8208S-8226S. https://doi.org/10.1177/15280837221094057/ASSET/IMAGES/LARGE/10.1177_15280837221094057-FIG11.JPEG